

Effects of Carrier Doping on Kinetic Parameters of CO₂ Hydrogenation on Supported Rhodium Catalysts

Zhaolong Zhang, Angelica Kladi, and Xenophon E. Verykios

Institute of Chemical Engineering and High Temperature Chemical Processes, Department of Chemical Engineering, University of Patras, GR-26500 Patras, Greece

Received October 25, 1993; revised March 1, 1994

A study of CO₂ hydrogenation on Rh/TiO₂ catalysts and of the influence of doping the TiO₂ carrier with W⁶⁺ cations on kinetic parameters has been conducted. It is found that while the reaction order with respect to H₂ and CO₂ partial pressures does not significantly change, the specific activity of CO₂ methanation is enhanced by up to 24 times upon doping the TiO₂ support with less than 1 at. % W⁶⁺ cations. A reduction of the apparent activation energy by ca. 25–34 kJ/mol and improvement of the stability of the catalytic performance are also observed by carrier doping. The greatly increased activity caused by doping is found not to be related to the SMSI phenomenon but to enhanced hydrogen adsorption capacity and weakening of the Rh–CO bond, as revealed by H₂ chemisorption measurements and infrared spectroscopic studies. The rate of gaseous CO formation is also found to be affected by carrier doping to a significant extent, via the alteration of surface CO coverage and of the strength of the M–CO bond. The intrinsic reason for the dependence of catalytic parameters upon doping of the carrier is discussed with respect to alterations of the electronic structure of the support upon doping, and electronic interactions between rhodium crystallites and the doped carrier. © 1994 Academic Press, Inc.

INTRODUCTION

It is well-known that an effective support not only provides a high surface area for metal dispersion but may also drastically modify the catalytic properties of the metal crystallites. The latter role of the support has attracted the attention of many researchers. Pioneering work on metal–support interactions has been conducted by Schwab [(1) and references therein], Solymosi (2), and Badour and Deibert (3), who attempted to investigate the electronic interaction at the metal–support interface which affects catalyst performance. One of the most documented discoveries of metal–support interactions is the strong metal–support interaction (SMSI) state of noble metals on reducible oxides such as TiO₂, Nb₂O₅, Ta₂O₅, and V₂O₅. Tauster *et al.* (4, 5) were the first to observe that noble metals supported on reducible oxides exhibited a complete suppression of hydrogen adsorption when they were reduced at high temperatures (≥ 773 K). Since then,

a large number of studies have been conducted on metal–support interaction phenomena. Several other kinds of metal–support interactions have been reported in the literature, and their origin, appearance, and effect on catalysis have been extensively studied (6–9).

Interest in this laboratory focuses on the effects of carrier doping on metal–support interactions, and on the study of the influence of such dopant-induced metal–support interactions on kinetic parameters of catalytic reactions (9–12). In the present study, the effect of doping TiO₂ carrier with W⁶⁺ cations on the metal–support interactions of the Rh/TiO₂ (W⁶⁺) catalyst system is investigated, employing CO₂ hydrogenation as a probe reaction. The interaction between metal and support, affected by carrier doping, was investigated earlier by Solymosi *et al.* (13), who found that while the Rh dispersion and H₂ adsorption capacity did not significantly change, the specific activity of CO and CO₂ hydrogenation were markedly varied by carrier doping. Renewal of this type of work in the present study is motivated by a recent finding that, without significant variation of metal dispersion, the quantity of H₂ and CO chemisorbed on supported Rh catalysts can be significantly enhanced, up to 4–10 times, by doping the TiO₂ support with a small amount of WO₃ (11). Such an effect of carrier doping on the chemisorptive behavior, which was not observed in previous studies (13), is of particular interest in the CO₂/H₂ reaction scheme.

TiO₂-supported rhodium catalysts exhibit very high activity in hydrogenation reactions. Previous studies have revealed that Rh/TiO₂ catalysts exhibit higher activity in CO or CO₂ hydrogenation as compared to Rh/SiO₂ and Rh/Al₂O₃ catalysts (13, 14). Although the reason for the high activity over Rh/TiO₂ is not yet fully understood, some results suggest that the enhanced activity for hydrogenation reactions over Rh/TiO₂ is related to the specific interaction between the TiO₂ carrier and the rhodium crystallites (15, 16); for instance, higher activities of CO hydrogenation were obtained over a Rh/TiO₂ catalyst in the SMSI state induced by reducing the catalyst at high temperatures (>773 K). The investigation of the effect of

doping of TiO₂ carrier and its influence on the hydrogenation reaction as well as its relation with the SMSI effect on this type of catalyst is therefore of industrial as well as of fundamental interest. The aim of the present study is twofold: (1) to investigate how the kinetic parameters of CO₂ hydrogenation are affected by the special properties of the doped catalysts, and (2) to better understand the nature of the effect of carrier doping on the metal-support interaction, particularly its relation with the well-known SMSI phenomenon.

EXPERIMENTAL

(a) Support and Catalyst Preparation

The parent titania carrier used in the present study was obtained from Degussa (P-25). To prepare the W⁶⁺-doped TiO₂ carriers, weighed amounts of TiO₂ and WO₃ (99% Alfa Products) were slurried with distilled water and thoroughly mixed. The water was evaporated under continuous stirring and the residue was dried at 373 K for 24 h. The dried residue was crushed and sieved and was then heated to 1173 K at a heating rate of 4 K/min. It was maintained at 1173 K for 5 h and was slowly cooled to room temperature. During this heat treatment the doping cation diffuses into the crystal structure of TiO₂ which is entirely transformed into the rutile form, as shown by XRD analysis.

Catalysts were prepared by the method of incipient wetness impregnation of the support with appropriate amounts of aqueous solutions of RhCl₃. Impregnated supports were dried at 373 K for 24 h. The resulting material was heated to 473 K at a heating rate of 5 K/min under nitrogen flow (50 cm³/min), and then reduced under H₂ flow (50 cm³/min) at 473 K for 2 h and subsequently at 523 K for 1 h. It was then cooled to 330 K under H₂ flow and under N₂ flow to room temperature.

The Rh content of the catalysts employed in the present study was invariably 0.5 wt%. The catalysts are designated as 0.5% Rh/TiO₂ (*x*%/W⁶⁺), where *x* is the dopant content of the carrier, in atom %.

(b) Kinetic Measurements

The apparatus employed for CO₂ hydrogenation rate measurements consisted of a flow measuring and controlling system, a tubular flow microreactor and an on-line analytical system. The flow rates of CO₂, H₂ and He were measured and controlled by thermal mass flow meters (MKS Instruments), and the flow streams were introduced into a mixing chamber prior to entering the reactor. The fixed-bed microreactor was a 1-cm-i.d. stainless-steel tube with 30 cm heating length. The catalyst, which was in the form of particles of diameters between 0.125 and 0.250 mm, was placed in the center of the reactor, supported

by glass wool. The catalyst particle size used in the present study was found experimentally not to offer any measurable intraparticle resistance in the transport of mass and heat. A thermocouple was used to measure the temperature along the axis of the reactor. In all cases, the temperature of the catalyst bed was found to be constant within ±1.0°C.

The reactor exit was connected on-line, via a gas sampling valve, with a gas chromatograph equipped with a thermal conductivity detector and a reporting integrator. A stainless steel (10' × 1/8") Carbosieve S-II 100/200 column was used to separate H₂, N₂, CO, CH₄, CO₂, C₂H₄, C₂H₆ and C₃ hydrocarbons. The CO₂/H₂ reaction was investigated in the temperature range 473–573 K. In most cases the feed consisted of 24% H₂, 6% CO₂, and 70% He (H₂/CO₂ = 4), on a molar basis. The total flow rate (50 ~ 100 cm³/min) and the amount of catalyst (0.4 ~ 0.6 g) were adjusted in order to operate the reactor in the differential mode. Prior to initiation of the reaction, the catalyst was pretreated in H₂ flow at 573 K for 1 h (at 773 K for 1 h for the SMSI experiment) and then cooled to the reaction temperature. Rate measurements were obtained after the system had reached steady state, which normally required 1–2 h. Between each set of measurements, the catalyst was exposed to H₂ flow for 30 min at the reaction temperature. Such a treatment was found to return the activity of the catalyst to its initial level.

(c) Infrared Spectroscopic Study

A Nicolet 740 FTIR spectrometer equipped with a DRIFT (Diffuse Reflectance Infrared Fourier Transform) cell was used for the present in situ measurements. The cell, containing ZnSe windows which were cooled by water circulating through blocks in thermal contact with the windows, allowed collection of spectra over the temperature range of 300–600 K at atmospheric pressure. For all spectra reported, a 32-scan data accumulation was carried out at a resolution of 3.0 cm⁻¹. During the measurements, external optics were continuously purged with dry nitrogen in order to minimize the level of water vapor and carbon dioxide in the testing chamber. An IR spectrum obtained under He flow at the reaction temperature was used as the background, to which each subsequent spectrum was ratioed.

Samples (50–70 mg) which had been previously finely powdered were placed onto the sample holder. The sample surface was carefully flattened in order to obtain high IR reflectivity. Before exposure to the reaction gas, the sample was pretreated at 573 K under H₂ flow for 30 min and then under He flow for 15 min. CO surface coverage is derived by normalizing the area of the CO band to the value for the catalyst saturated with 76 Torr CO at 375 K. At this temperature, both the Boudouard reaction (CO

disproportionation) and the oxidative disruption of Rh–Rh bonds, induced by CO, are not significant.

RESULTS

The effects of carrier doping on metal-support interactions were investigated over the Rh/TiO₂ ($x\%$ W⁶⁺, $x = 0, 0.11, 0.22, 0.45,$ and 0.67) catalysts, employing CO₂ hydrogenation as a probe reaction. In particular, the influence of dopant concentration on kinetic parameters of CO₂ hydrogenation such as activity, selectivity, stability, apparent activation energy, and reaction order with respect to CO₂ and H₂ were investigated. The surface species formed over the doped and undoped catalysts during CO₂ hydrogenation were studied by *in situ* FTIR spectroscopy. The possible relationship between the phenomenon of metal–support interaction induced by carrier doping and the SMSI phenomenon was also investigated for this catalyst system.

(a) Effects of Carrier Doping on Kinetic Parameters of CO₂ Hydrogenation

(a1) *Activity and selectivity.* The effect of dopant concentration in the carrier matrix ($x = 0, 0.11, 0.22, 0.45,$ and 0.67 at.%) on the activity of Rh for CO₂ hydrogenation, in the form of turnover frequencies of the methanation and CO formation reactions, is shown in Figs. 1 and 2, respectively. The turnover frequencies (TOF) of doped and undoped catalysts are estimated on the basis of metal dispersion of the corresponding undoped catalyst since the dispersion of the doped catalysts cannot be directly estimated due to their abnormal hydrogen adsorption capacity. Doping of the support with very small amounts of W⁶⁺ cations (<1 at.%) is not expected to cause significant alterations in Rh particle size. Earlier work by Solymosi

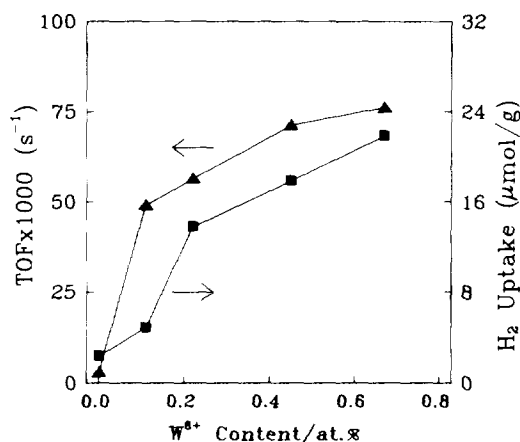


FIG. 1. The dependence of H₂ uptake (at 300 K) and specific activity for CO₂ methanation (at 508 K) of Rh on the concentration of W⁶⁺ dopant in the TiO₂ carrier.

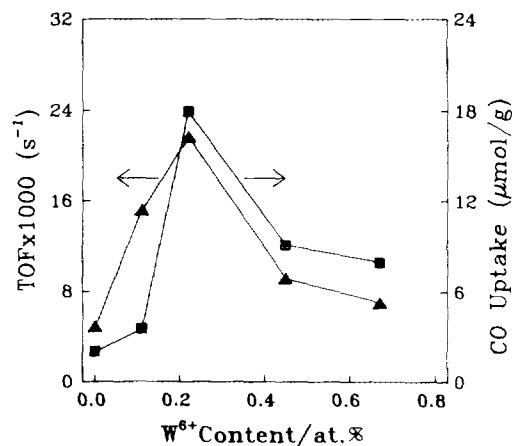


FIG. 2. The dependence of CO uptake (at 300 K) and specific activity for CO formation (at 508 K) of Rh on the concentration of W⁶⁺ dopant in the TiO₂ carrier.

et al. (13) showed that carrier doping does not significantly alter the dispersion of supported Rh. In recent studies carried out in this laboratory, the dispersion of rhodium on the doped supports was also found, by TEM analysis (11) and by *in situ* XPS measurements (based on the ratios of $I_{\text{Rh}}/I_{\text{Ti}}$ for the doped and undoped catalysts), not to be significantly different from that on the undoped carrier.

It is apparent (Fig. 1) that the activity of Rh for CO₂ methanation is drastically enhanced (by up to 24 times) when Rh is dispersed on W⁶⁺-doped TiO₂ carriers. The degree of enhancement is a function of dopant concentration in the carrier, especially at low concentration levels. It is also interesting to note that a significant amount of CO, which has been proposed as an important intermediate of CO₂ hydrogenation (17, 18), is observed over the entire series of catalysts (Fig. 2). Unlike the case for methane formation, the rate of CO formation does not increase monotonically with increasing dopant concentration. The rate is shown to pass through a maximum at a dopant content of 0.22 at.% (Fig. 2). At this level of doping, the TOF of CO formation is approximately eight times larger than that observed over the undoped catalyst. The CO selectivity over the undoped catalyst amounts to ca. 45%, while less than 10% selectivity of CO is observed over the doped catalysts. This suggests that carrier doping affects the Rh surface electronic states, which leads to enhancement of methanation activity, much more drastically than it does CO formation activity.

The H₂ and CO equilibrium adsorption capacity (at 298 K) of this series of catalysts, as obtained in a previous study (11), is also illustrated in Figs. 1 and 2, respectively. The H₂ adsorption capacity of Rh increases monotonically with increasing W⁶⁺-dopant concentration in the carrier (Fig. 1), while the CO adsorption capacity goes through a maximum at a level of doping of 0.22 at.% (Fig. 2).

Based on a recent spectroscopic study in this laboratory (19), the enhanced H_2 adsorption capacity is attributed to multiple adsorption (e.g., one surface Rh atom adsorbing two hydrogen atoms) and to hydrogen spillover from the Rh crystallites to the carrier, the latter being the dominant mechanism. Due to higher-valence doping of the carrier, numerous cationic vacancies are formed on the surface of the carrier, which favorably associate with spilled over hydrogen atoms, probably in the form of OH^- groups. The alteration of the CO adsorption capacity is related to the disruption of the Rh–Rh bonds of the Rh crystallites, induced by CO, and formation of the gem-dicarbonyl $Rh^+(CO)_2$ species, as revealed by infrared studies (19). The extent of the Rh–Rh bond disruption is affected by doping of the carrier, probably via electronic interactions between the metal crystallites and the carrier. It must be emphasized, however, that under CO_2 hydrogenation conditions Rh–Rh disruption induced by CO does not take place. As will be shown in a subsequent section, no gem-dicarbonyl species is observed over the working catalyst surface. This observation, along with TEM results reported earlier (11), shows that carrier doping does not significantly influence the Rh particle size of the working catalyst.

The variation of the activity of Rh/TiO_2 ($x\% W^{6+}$) catalysts with time on stream was examined at 573 K. It was found that the activity of the undoped catalysts decreases with time on stream and reaches a relatively stable level (ca 80% of initial level) after approximately 2 h. For the doped catalysts ($x = 0.11$ and 0.22 at.%) the activity was found to increase slightly with time on stream and a constant activity was reached within 1 h. The activity becomes essentially time-independent when the dopant concentration is high ($x = 0.45$ and 0.67 at.%). Apparently, doping of the TiO_2 carrier with W^{6+} cations improves the stability of the catalytic performance. Improvement of the stability of catalytic performance by altrivalent cation doping of the support has also been observed over the 0.5% Pt/doped- TiO_2 catalysts for the CO hydrogenation and water–gas shift reactions (20).

(a2) *Apparent activation energy.* The temperature sensitivity of the CO_2 hydrogenation reaction was investigated within the temperature range 473–573 K and typical Arrhenius-type plots of the methanation reaction are shown in Fig. 3. The apparent activation energies of CO_2 methanation of doped and undoped catalysts are estimated from these plots and the results are presented in Table 1, in which the corresponding apparent activation energies of CO formation are also included.

Over the undoped catalyst, an apparent activation energy of ca 103 kJ/mol is found for CO_2 methanation. This value is close to that obtained in a previous study over a Rh/TiO_2 catalyst (13). An apparent activation energy of

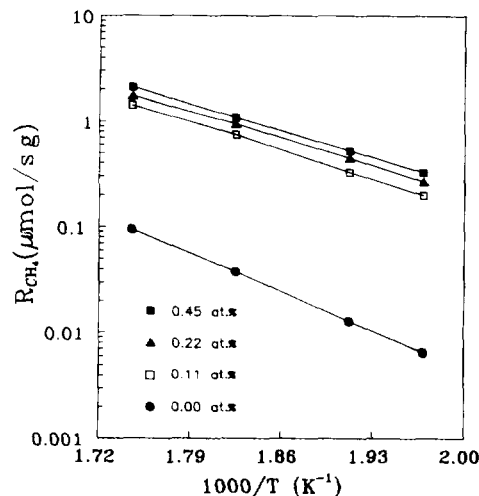


FIG. 3. Influence of temperature on CO_2 methanation activity of the 0.5% Rh/TiO_2 ($x\% W^{6+}$) catalysts. $T = 500$ – 600 K; $H_2/CO_2 = 4$.

ca 55 kJ/mol is found for CO formation over the undoped catalyst. This value is much lower than that for CO_2 methanation, indicating that the dissociation of CO_2 to CO is much easier, as compared to the methanation of CO_2 . A reduction in the apparent activation energy of methane formation by approximately 25–34 kJ/mol is observed when rhodium is dispersed on W^{6+} -doped TiO_2 carriers. The reduction in apparent activation energy does not seem to depend on dopant concentration (see Table 1). A reduction of the apparent activation energy by ca. 13–25 kJ/mol is also observed for CO formation when rhodium is dispersed on doped carriers. It seems that doping of the TiO_2 carrier enables the reaction of CO_2 to CO and CH_4 to proceed through schemes with lower energetic barriers over the supported Rh crystallites.

(a3) *Reaction order with respect to reactants.* The influence of the partial pressure of reactants on the rate of CO_2 hydrogenation over the doped catalysts was investigated at 508 K. For comparison, the same influence over the undoped catalyst was also examined. However,

TABLE 1

Effect of Carrier Doping on the Apparent Activation Energy for CO_2 Hydrogenation on 0.5% Rh/TiO_2 ($x\% W^{6+}$) Catalysts

x (at.%)	E_{CH_4} (kJ/mol)	E_{CO} (kJ/mol)
0	102.8	54.8
0.11	78.2	28.8
0.22	74.4	42.6
0.45	69.4	26.3
0.67	70.6	25.9

temperature was raised to 573 K, in order to obtain comparable conversions. It should be mentioned that the dependence of the rate of CO formation on reactant composition has not been studied in detail in the literature. Although gaseous CO is only a by-product of the conversion of CO₂ to hydrocarbons, the variation of its formation rate with the partial pressure of the reactants may provide important information for elucidating the surface schemes, since adsorbed CO is proposed to be an intermediate species during CO₂ hydrogenation.

The influence of CO₂ and H₂ partial pressures on the rate of CH₄ and CO₂ methanation is shown in Figs. 4 and 5, respectively. Following a power-law formulation of the type

$$R_{\text{CH}_4} = k_{\text{CH}_4} \cdot P_{\text{CO}_2}^{n_1} \cdot P_{\text{H}_2}^{m_1}, \quad [1]$$

zero-order dependence of the methanation rate on CO₂ partial pressure is obtained (Fig. 4), and near half-order dependence of the methanation rate on H₂ partial pressure can be derived, although the order with respect to P_{H_2} appears to increase slightly with increasing dopant concentration (Fig. 5).

The influence of CO₂ and H₂ partial pressure on the rate of CO formation is illustrated in Figs. 6 and 7, respectively. First-order dependence of CO formation on CO₂ partial pressure can be derived according to the power-law formulation. However, the dependence of CO formation rate on H₂ partial pressure seems to be complicated and not to conform to a rate expression of the type of Eq. [1]. The rate increases linearly at low H₂ pressures ($P_{\text{H}_2} = 0 \sim 50$ Torr), decreases at intermediate H₂ pressures ($P_{\text{H}_2} = 50 \sim 200$ Torr), and is essentially independent of H₂ pressure when this exceeds 300 Torr (Fig. 7). Several typical kinetic equations have been used in the

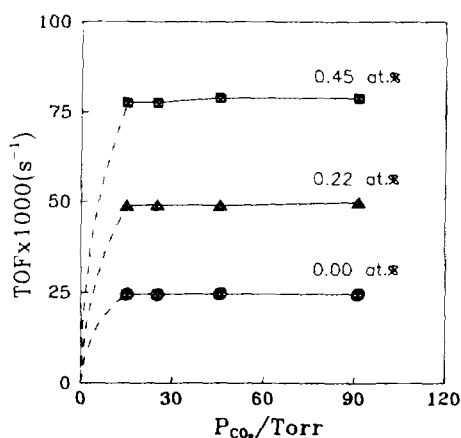


FIG. 4. The influence of the partial pressure of CO₂ on the rate of methane formation. $P_{\text{H}_2} = 182$ Torr; $P_{\text{CO}_2} = 20 \sim 70$ Torr; balance He. $T = 508$ K for the doped catalysts; $T = 573$ K for the undoped catalyst.

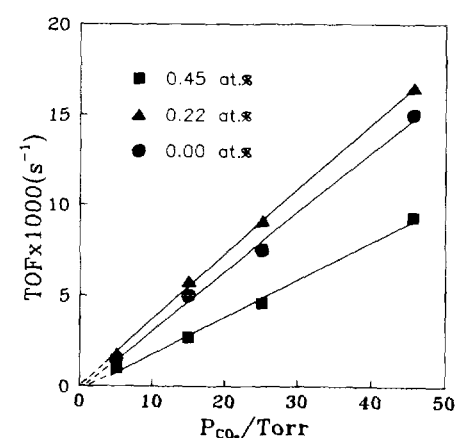


FIG. 6. The influence of the partial pressure of CO₂ on the rate of CO formation. $P_{\text{H}_2} = 182$ Torr; $P_{\text{CO}_2} = 20 \sim 70$ Torr; balance He. $T = 508$ K for the doped catalysts; $T = 573$ K for the undoped catalyst.

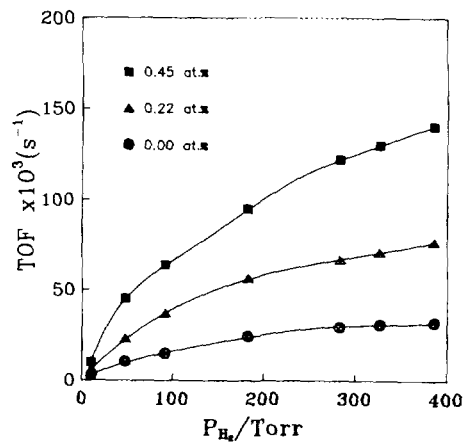


FIG. 5. The influence of the partial pressure of H₂ on the rate of methane formation. $P_{\text{CO}_2} = 46$ Torr; $P_{\text{H}_2} = 0 \sim 400$ Torr; balance He. $T = 508$ K for the doped catalysts; $T = 573$ K for the undoped catalyst.

data-modelling study, and the following equation gave the best fit:

$$R_{\text{CO}} = k_{\text{CO}} \cdot P_{\text{CO}_2}^{n_2} \cdot P_{\text{H}_2}^{m_2} / (1 + CP_{\text{H}_2}^{m_3}). \quad [2]$$

Here C is a constant and n_2 , m_2 , and m_3 are variables which are marginally affected by the concentration of the dopant. The above equation does not have a direct physical meaning, but it suggests that the reaction of CO formation does not follow the Langmuir–Hinshelwood scheme. This reaction route involves adsorption and hydrogen-assisted decomposition of CO₂ to adsorbed CO which then desorbs, at a low rate (slow step) to the gas phase. If a Langmuir–Hinshelwood reaction scheme was followed, the partial pressure of carbon monoxide, instead of the partial pressure of hydrogen, should appear in the denominator of the derived equation (the adsorption of

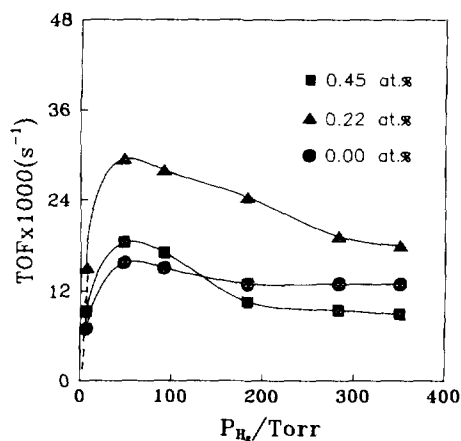


FIG. 7. The influence of the partial pressure of H_2 on the rate of CO formation. $P_{CO_2} = 46$ Torr, $P_{H_2} = 0 \sim 400$ Torr; balance He. $T = 508$ K for the doped catalysts; $T = 573$ K for the undoped catalyst.

carbon monoxide is much stronger than that of hydrogen). At high hydrogen partial pressure, methanation of adsorbed CO is favored, at the expense of CO desorption. This competitive process inhibits the rate of gas-phase CO production and gives rise to the denominator of Eq. [2].

The orders with respect to the partial pressures of CO_2 and H_2 are summarized in Table 2. It is shown that doping of the carrier does not significantly alter the order of either reaction.

(b) Infrared Spectroscopic Study

The CO_2/H_2 reaction over the Rh/TiO₂ and Rh/TiO₂(W⁶⁺) catalysts was also investigated by in situ infrared spectroscopy at 508 K. Spectral features at ca. 1570, 1650, 2044–2058, and 1880–1900 cm^{-1} were observed. The bands at ca. 1570 cm^{-1} correspond to the formate species, most probably on the carrier (21), while the weak band at ca. 1650 cm^{-1} (some noise may be due to the presence of water vapor which is produced in the reaction)

TABLE 2

Reaction Orders with Respect to Partial Pressures of CO_2 and H_2 over the 0.5% Rh/TiO₂ ($x\%$ W⁶⁺) Catalysts

Order ^a	Dopant (at.%)		
	0	0.22	0.45
n_1	0	0	0
n_2	1.0	1.0	1.0
m_1	0.49	0.50	0.53
m_2	1.1	0.92	0.95
m_3	1.2	1.2	1.0

^a For the designations of n_1 , n_2 , m_1 , m_2 , and m_3 , see Eqs. [1] and [2].

may correspond to carbonate species on the surface (22). Since the surface area of the carriers studied is rather small (<10 m^2/g), the formate bands are much weaker as compared to those observed on the catalyst with high carrier surface area (usually >50 m^2/g) (21). The spectral features at ca. 2044–2058 cm^{-1} and ca. 1880–1900 cm^{-1} are due to the formation of the linear and the bridged adsorbed CO on the rhodium surface, respectively, and are shown in Fig. 8 for the undoped and the 0.67 at.% W⁶⁺ doped catalysts. The twin bands of the gem-dicarbonyl species at ca. 2090 and 2035 cm^{-1} , which are typically surface species resulting from CO adsorption on rhodium crystallites at low temperatures (23), are not observed on either catalyst, under the CO_2/H_2 reaction conditions. These observations are essentially in agreement with those reported previously on Rh/Al₂O₃ and Rh/TiO₂ catalysts (24–26). It is noted that the band of the linearly adsorbed CO is unsymmetric. It contains a shoulder at around 2030 cm^{-1} . Probably, the component at lower vibrational frequency is due to the formation of Rh carbonyl hydride, as proposed earlier (24, 27). An interesting phenomenon revealed in the present infrared study is the frequency shift of the band due to the linearly adsorbed CO on the Rh surface, from 2044 cm^{-1} on the undoped carrier to 2058 cm^{-1} on the doped one (the weak band of the bridged adsorbed CO is rather broad, and any shift due to doping cannot be distinguished). Also, the CO coverage on the working catalyst surface is found to be reduced from ca 0.30 on the undoped catalyst to 0.16 on the doped catalyst (Fig. 8). It is known (24, 26) that an increase of CO coverage results in a frequency shift of the CO band towards higher wavenumbers. The present blue shift of the CO band is observed over the doped catalyst which has a lower CO coverage, as compared to that of the undoped catalyst. Therefore, the blue shift

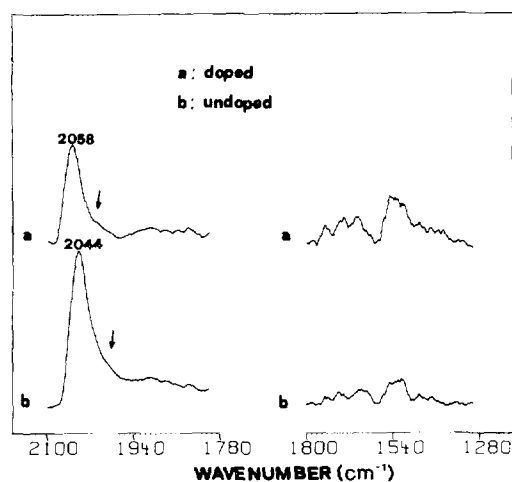


FIG. 8. Infrared spectra of adsorbed CO and formate species formed during CO_2 hydrogenation at 508 K and $H_2/CO_2 = 4$ on (a) 0.5 wt% Rh/TiO₂ (0.67 at.% W⁶⁺) catalyst and (b) 0.5 wt% Rh/TiO₂ catalyst.

which is observed upon carrier doping is not due to the alteration of the CO coverage. The variation of the C–O vibrational frequency and CO coverage upon carrier doping is discussed in a subsequent section, with respect to the enhanced activity of CO₂ methanation.

(c) *The Possible Relationship between the Effects of Doping of the Support and the SMSI State*

In order to assess whether the significant enhancement in the rate of CO₂ methanation by doping the TiO₂ support is related to the occurrence of the SMSI state, a 0.5 wt.% Rh/TiO₂ (0.22 at.% W⁶⁺) catalyst was reduced at high temperature (773 K) in H₂ flow for at least 2 h, and the activity of the resulting catalyst is compared to that of the same catalyst reduced at low temperature (i.e., at 523 K). Since the morphology of the surface may change during high temperature reduction, the TOF cannot be safely derived for the catalyst in the SMSI state. Therefore, instead of using TOF, activity is expressed in $\mu\text{mol/g}\cdot\text{catalyst}/\text{s}$.

Figure 9 shows the variation of the activity of CO₂ hydrogenation over the SMSI catalyst with reaction time. As compared to the activity of the catalyst in the non-SMSI state (i.e. reduced at 573 K), the initial total activity of the catalyst in the SMSI state (i.e. reduced at 773 K) is approximately 50% lower. While the initial activity for methane formation is almost totally suppressed, the initial activity for CO formation is significantly enhanced, compared to that of the non-SMSI state catalyst. The different influence of the SMSI state on CO and CH₄ formation reveals that the reactions of CO and CH₄ formation proceed over different types of reaction sites.

A gradual reversal of the SMSI state is witnessed as

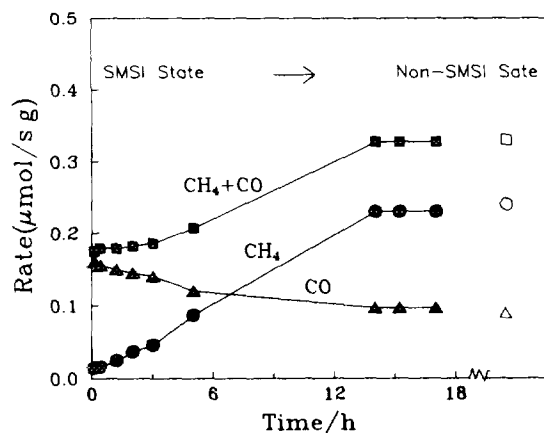


FIG. 9. Variation of the activity of the 0.5% Rh/TiO₂ (0.22% W⁶⁺) catalyst reduced at 773 K as a function of reaction time. The unfilled symbols, shown on the right side, are data obtained from the 0.5% Rh/TiO₂ (0.22% W⁶⁺) catalyst reduced at 573 K. Reaction conditions: $T = 508\text{ K}$; $\text{H}_2/\text{CO}_2 = 4$; balance He.

TABLE 3

Effect of SMSI on the Activation Energy and Reaction Rate on 0.5% Rh/TiO₂ (0.22% W⁶⁺) Catalyst

State	E_{CH_4} (kJ/mol)	E_{CO} (kJ/mol)	$R_{\text{CH}_4}^a$ ($\mu\text{mol}/\text{s g}$)	R_{CO}^a ($\mu\text{mol}/\text{s g}$)
SMSI	89.9 ± 8.0	39.7 ± 8.0	0.015	0.16
Non-SMSI	74.4 ± 2.0	42.6 ± 2.0	0.23	0.063

^a The rate was obtained at 508 K, with a H₂/CO₂ ratio of 4.

reaction time increases (see Fig. 9). Within the first hour on stream, only less than 10% of reversal is observed. A stable activity is observed after exposing the catalyst to reaction conditions for more than 10 h. As shown in Fig. 9, the activity obtained from the catalyst reduced at 773 K approaches that of the catalyst reduced at 573 K (shown by the unfilled symbols), when the time on stream is over 10 h. This indicates that the SMSI state can be fully reversed by exposing the catalyst to CO₂/H₂ reactant mixture. The gradual reversal of the SMSI state may be due to the presence of water vapor, a product of the CO₂ hydrogenation reaction, and/or oxygen atoms which may arise from the dissociation of CO₂. Both water vapor and surface oxygen adatoms have been reported to be capable of destroying the SMSI state (28, 29).

Since the SMSI state of the doped catalyst is slowly reversed within the first several hours of reaction time, some meaningful kinetic studies could be carried out over the catalyst in the "pseudo-SMSI" state. The results showed that the values of the reaction order with respect to H₂ and CO₂ in the SMSI state were close to the corresponding ones obtained in the non-SMSI state. The apparent activation energies of the methanation reaction obtained for the catalysts in the SMSI and non-SMSI states were found to be rather different, whereas those for the CO formation were found to be approximately the same. These values are compared in Table 3. When the catalyst is brought into the SMSI state, an increase in apparent activation energy for methanation by ca 17 kJ/mol is observed, whereas the apparent activation energy for CO formation is only slightly changed from ca 43 to ca 39 kJ/mol.

DISCUSSION

(a) Influence of Carrier Doping on Kinetic Parameters

The effects of carrier doping on kinetic parameters of CO₂ hydrogenation, i.e., specific catalytic activity, selectivity, activation energy, and reaction orders with respect to the reactants, were presented in a previous section. As discussed above, the metal dispersion of the working catalyst is hardly affected by doping TiO₂ with W⁶⁺ cat-

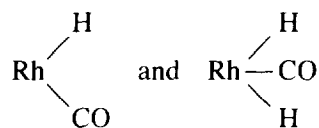
ions. Therefore, the observed variations of the kinetic parameters with doping of the carrier are attributed to changes in the electronic properties of the catalysts, rather than to geometric parameters. The abnormal chemisorptive behavior of the doped catalysts, revealed by the chemisorption of H_2 at room temperature (see Fig. 1), should be related to changes in the electronic properties of the catalysts induced by carrier doping. Although, under reaction conditions, such differences in H_2 chemisorptive capacity between the doped and undoped catalysts may be changed, as compared to those observed at room temperature, in all probability the same tendency does remain. This tendency should, in some way, be related to the alterations in the kinetic parameters of CO_2 hydrogenation. To this end, the reaction rate of CO_2 hydrogenation is compared with the quantity of H_2 chemisorbed at equilibrium on the surface. Figure 1 shows the dependences of the methanation rate and hydrogen uptake on the dopant content of the carrier. A good correlation seems to exist between these two parameters, indicating that the enhancement of the rate of CO_2 methanation with carrier doping might be related to higher chemisorptive capacity of hydrogen of the doped catalysts. The relation between the rate of CO_2 methanation and H_2 chemisorptive capacity will be further discussed later with respect to the competitive adsorption of CO.

Adsorbed CO has been proposed to be an important intermediate species during CO_2 hydrogenation (17, 18). The observation of gaseous CO over the catalysts studied suggests that CO partly desorbs from the surface. If the conversion of CO_2 to CO is assumed to be a fast step (21), then the rate of CO formation would be governed by the rate of desorption of the adsorbed CO, which is a function of surface coverage and of the strength of the M -CO bond. This reasoning is derived from the fact that the rate of CO formation does not follow the Langmuir-Hinshelwood reaction scheme, which assumes that the surface reaction is the rate-determining step. Presumably, the gaseous CO originates mainly from the surface CO which is weakly adsorbed. Supposing that the coverage of the weakly adsorbed CO is in direct proportion to the quantity of CO uptake at room temperature (a temperature at which the weakly adsorbed CO does not desorb), then the rate of CO formation should be related to the CO uptake. To verify this hypothesis, the dependences of the rate of CO formation and CO uptake at room temperature versus the concentration of W^{6+} dopant are plotted in Fig. 2. It is seen that the two dependences exhibit a similar pattern; i.e., the catalyst with high CO uptake exhibits a high rate of CO formation. Thus, it follows that the effect of doping on the rate of CO formation is related to the alteration of the coverage of CO which is relatively weakly adsorbed.

In addition to the variation of CO uptake at room tem-

perature, the Rh-CO bonding is also affected by carrier doping. As shown by infrared results (Fig. 8), a blue shift by ca 14 cm^{-1} of the CO band is witnessed over the doped catalyst. According to the Blyholder-Dewar-Chatt model (30, 31), the bonding of CO to a metal surface occurs through formation of a σ -bond by overlapping of an empty d orbital and a lone electron pair on the carbon atom of CO, and formation of a π -bond between a filled metal d orbital and an empty antibonding orbital ($2\pi^*$) of CO. The observation of strengthening of the C-O bond on the doped catalyst, as indicated by the blue shift, implies that either the σ -bonding or the π -bonding or both, between Rh metal and CO are less effective, i.e., weakening of the Rh-CO bonding. The smaller CO coverage on the doped catalyst under reaction conditions (Fig. 8) can thus be ascribed to the weakening of the Rh-CO bond, which leads to partial desorption of adsorbed CO. In an earlier CO-TPD study conducted in this laboratory (11), it was also found that the temperature for CO desorption from supported Rh was shifted to lower values by doping of TiO_2 with W^{6+} cations, indicating weakening of the Rh-CO bond. It should also be mentioned that the enhanced H_2 adsorption capacity upon carrier doping is interrelated with the weakening of the Rh-CO bond. Although the coverage of hydrogen on the working catalyst surface is expected to be much smaller than that of CO, the weakening of the Rh-CO bond favors the increase of hydrogen coverage.

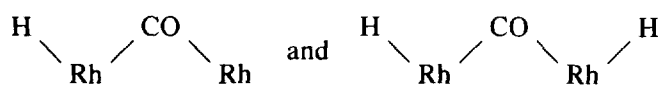
The reduction of the apparent activation energy of CO_2 methanation upon carrier doping is another factor promoting methane formation. This reduction suggests that H-assisted CO dissociation, the rate determining step for CO_2 methanation (17), is favored on the doped catalyst. As a first approach, this appears to contradict the infrared results which show strengthening of the C-O bond upon carrier doping. However, since C-O dissociation is a slow step, the majority of the adsorbed CO accumulated on the working catalyst surface actually does not instantaneously participate in the reaction scheme. Thus, only a small fraction of the adsorbed CO instantaneously participates in the methanation process, while the majority of it is only a "surface poison," in view of the competitive adsorption with hydrogen. By weakening the Rh-CO bond via carrier doping, the hydrogen coverage is expected to be increased. The higher hydrogen coverage on the doped catalyst favors the formation of Rh carbonyl hydride species which consists of a Rh carbonyl complex and one or two hydrogen atoms associated to CO via the Rh center (17, 24):



Due to charge transfer from the bonded hydrogen to the Rh center, the π -donation from Rh into an antibonding π -orbital of CO is enhanced. Consequently, the C–O bond is significantly weakened whereas the Rh–CO bonding is strengthened. Through this mechanism, the C–O dissociation is much easier, as compared to the dissociation without hydrogen assistance, which is reflected in lower activation energies of the CO₂/H₂ reaction scheme. This is equivalent to saying that two types of adsorbed CO species exist on the working catalyst surface, the carbonyl species which is relatively weakly adsorbed and the carbonyl hydride species which is strongly adsorbed. The weakening of the Rh–CO bond of the Rh carbonyl species (which is in abundance) by carrier doping would favor the enhancement of hydrogen coverage, by which the formation of the Rh carbonyl hydride species is promoted. The fact that a shoulder is detected at lower frequencies of the main CO band (Fig. 8) suggests the formation of Rh carbonyl hydride on the present catalysts. Unfortunately, the position and concentration of Rh carbonyl hydride species cannot be precisely evaluated due to overlapping of the bands of the Rh carbonyl complex (at 2044–2058 cm⁻¹) and the Rh carbonyl hydride complex (at ca. 2030 cm⁻¹). It is recalled that in a study of CO and CO₂ hydrogenation over Ni catalyst reported by Fujita *et al.* (32), it was shown that the formation of methane is enhanced by ca. 20 times if the adsorbed CO formed during reaction is manipulated to be partially removed in a TPD manner. Also, it is well-known (25, 33) that CO₂ hydrogenation is effectively inhibited by adding a small amount of gaseous CO, which tends to increase the CO coverage on the surface.

Based on the above arguments it may be concluded that the influence of carrier doping on activity for CO₂ hydrogenation is related to weakening of the Rh–CO bond which results in two factors promoting methane formation: one is the increased hydrogen coverage, which enhances methane formation by increasing the concentration of H intermediate species participating in the rate determining step; the other is the enhanced extent of formation of Rh carbonyl hydride which lowers the activation energy of C–O dissociation.

An alternative explanation for the effect of carrier doping on CO₂ methanation is the consideration of the bridged-bonded CO as the reactive intermediate, as proposed earlier by Solymosi *et al.* over Pd catalysts (34). The weakening of the Rh–CO bond of the linearly bonded CO species (consisting of the majority of the surface CO species) would favor the formation of bridged Rh carbonyl-hydride species:



via the enhancement of hydrogen coverage. The dissociation of CO and the rate of methane formation is also expected to be enhanced if this mechanism is operable.

The reduction of the apparent activation energy for CO formation upon carrier doping implies that the energy for CO desorption is reduced, since the rate of CO formation is approximately equivalent to the rate of CO desorption (the conversion of CO₂ to CO in the presence of hydrogen is a fast step (21)). This is in agreement with the infrared results which suggest that the Rh–CO bond is weakened by carrier doping. The fact that the apparent activation energy for CO formation (25–55 kJ/mol) is much lower than that for CO₂ methanation (70–103 kJ/mol) suggests that the rate determining step for CO₂ methanation is not the conversion of CO₂ to CO but a subsequent step during the further hydrogenation of CO to methane, if the view that adsorbed CO is an intermediate species in the CH₄ formation route is accepted.

Recent results obtained in this laboratory (12) showed that the rate of CO hydrogenation and the apparent activation energy of the reaction were also reduced by carrier doping. Comparatively, the apparent activation energy of CO₂ hydrogenation (71–103 kJ/mol) is somewhat smaller than that corresponding to CO hydrogenation (103–125 kJ/mol), while the rate of CO₂ hydrogenation is higher than the rate of CO hydrogenation. Since the dissociation of adsorbed CO is believed to be the rate-determining step for both CO and CO₂ hydrogenation, the differences in the reaction rate and the apparent activation energies between the two hydrogenation reactions over the Rh/TiO₂ (W⁶⁺) catalysts may suggest that the extent of formation of the metal carbonyl-hydride species on the catalyst is different, possibly due to the different hydrogen coverages under CO and CO₂ hydrogenation, although both reactions may proceed via the same adsorbed CO intermediate. In view of strong adsorption of CO, as compared to adsorption of CO₂, the above deduction is reasonable since higher coverage is expected in the case of CO₂ hydrogenation.

It is interesting to note that while the activity and the coverage of surface species are significantly affected by carrier doping, the reaction orders with respect to the partial pressure of reactants are not altered to any significant extent. This suggests that doping of the carrier only alters the extent of existing surface processes for methane formation, but does not create new reaction pathways. The zero-order dependence of CO₂ methanation on CO₂ partial pressure (Fig. 4) can be explained by the "buffering effect" of high CO surface coverage (21). As indicated by the present IR results, the surface CO coverage is as high as 0.16–0.3. The presence of such high CO coverage itself means that the conversion of CO₂ to adsorbed CO is fast, while the further hydrogenation of the adsorbed CO is a slow step. As a reasonable deduction, it is ex-

pected that the rate of CO₂ methanation is independent of CO₂ partial pressure since even at low CO₂ partial pressures, the rate of formation of adsorbed CO is sufficiently larger than the rate of methanation. The observation of near first-order dependence of CO formation on CO₂ partial pressure (Fig. 6) means that the fraction of the surface CO which desorbs into the gas phase increases linearly with increasing CO₂ partial pressure. A larger CO pool is expected on the surface when a higher CO₂ partial pressure is applied due to the rapid conversion of CO₂ to CO and the slow hydrogenation of CO. Presumably, the fraction of the weakly adsorbed CO is also increased, and the rate of CO formation is enhanced.

The dependence of CO formation rate upon H₂ partial pressure (Fig. 7) may be related to the existence of two effects of hydrogen on the formation of adsorbed CO. The first is that the formation of the CO intermediate from CO₂ is assisted by hydrogen, probably via the formation of formate-type species with subsequent decomposition of this species (17). The formation of formate species is observed in the present in situ IR study. The second is that the CO intermediate is reacted with hydrogen to form methane (i.e., a decrease in the concentration of the CO species). At low hydrogen partial pressures, the former effect dominates, resulting in the increase of CO formation with increasing hydrogen partial pressure. The latter effect becomes increasingly important upon increasing hydrogen partial pressure. This eventually leads to a decrease of CO coverage, and, consequently, to the decrease of the rate of CO formation.

The nearly half-order dependence of the methanation rate upon H₂ partial pressure (Fig. 5) suggests that the rate of methanation depends linearly on the concentration of adsorbed hydrogen, which is in equilibrium with gaseous H₂ via a dissociative adsorption process. This implies that the rate of methanation is enhanced by increasing the hydrogen coverage on the working catalyst. This deduction exactly fits the tendency showed in Fig. 1, in which a good correlation between activity and H₂ chemisorption capacity is shown.

(b) Interpretation of the Effect of Doping the Support

In the discussion above, alterations in the chemisorptive and catalytic behavior of the supported Rh crystallites are attributed to changes in the surface electronic states, caused by carrier doping. The model used to interpret these alterations is based on the theory of metal–semiconductor contacts (Schottky junctions). According to this theory, the Fermi energy levels of a metal and a semiconductor in contact are at equal heights when thermodynamic equilibrium is achieved. This requirement results in electron transfer between the two solids, the direction of which depends on the initial (before contact) work

functions of the two solids. Reduced TiO₂ has a work function of ca. 4.6 eV (35), which is lower than that of pure Rh metal (amounting to ca. 5.0 eV) (36). As a result, charge is being transferred from the TiO₂ carrier to the Rh crystallites until the Fermi energy levels of the two materials in contact are at the same height. Doping of TiO₂ with higher valence cations, such as W⁶⁺, enhances the *n*-type semiconductivity of the material and lowers the activation energy of electron conduction, as has been demonstrated experimentally (9, 20). This corresponds to further lowering of the work function of TiO₂, which results in the intensification of the charge transfer from the doped TiO₂ to the Rh crystallites. The enhanced transfer of electrons from the doped TiO₂ carrier to the supported Rh crystallites may lead to electronic alterations of the supported Rh particles and the catalyst surface (11, 12). This weakens the Rh–CO bond, which is accompanied by strengthening of the C–O bond, as evidenced by IR results.

(c) Comparison of the Effects of SMSI and of Doping the Support

The SMSI effect on CO₂ hydrogenation is significant in the present catalyst system (see Fig. 9). The reduction of the rate of CO₂ methanation due to the high temperature reduction of the catalyst may be a result of the modification of the surface morphology, e.g. the migration of TiO_x entities onto the metal surface, a phenomenon related to the SMSI state. The migration of TiO_x entities onto the metal surface may block the metallic sites required for the hydrogenation of adsorbed CO. The reversal of the SMSI state caused by CO₂ hydrogenation implies that the working catalyst surface during CO₂ hydrogenation is free of the site-blocking oxide species. Even if some site-blocking oxide species are preintroduced during the high-temperature reduction, they are removed by exposing the catalyst to the CO₂ hydrogenation reaction conditions. Moreover, as has been demonstrated earlier (13, 17) and in this work, the attainment of high activity of supported Rh catalysts does not require high-temperature reduction. Thus, it is safe to conclude that the present drastic enhancement in the activity of CO₂ hydrogenation, caused by doping of TiO₂ with W⁶⁺ cations, has nothing to do with the SMSI phenomenon. The differences of CO₂ hydrogenation between the non-SMSI and the SMSI states are also reflected in the different influences on apparent activation energy for CO₂ methanation (see Tables 1 and 3).

In contrast to the formation of methane which is unfavorable in the SMSI state, the production of CO is enhanced when the SMSI state is induced (see Fig. 9). Apparently, the two reactions proceed over significantly different reaction sites. Unlike the conversion of adsorbed

CO to methane, the formation of adsorbed CO from CO₂ occurs at the metal-support interface (21). A migration of TiO_x entities onto the metal surface would be expected to produce more interfacial sites on the surface. This certainly gives a positive effect on CO formation.

It is noted that a similar kinetic variation of CO₂ hydrogenation induced by the SMSI effect has recently been observed over a Rh/TiO₂ catalyst (37); i.e., the rate of CO formation increased, whereas the rate of CH₄ formation decreased. However, unlike the present results over the doped catalyst, a gradual reversal of the SMSI state was not observed over the Rh/TiO₂ catalyst (38). The discrepancy between the Rh/TiO₂ and the Rh/TiO₂(W⁶⁺) catalysts should be due to the different properties of the supports, probably because of the higher electric conductivity of the W⁶⁺-doped TiO₂, which favors the reversal of the SMSI state of the supported Rh catalyst, as in the case of Rh/Nb₂O₅ (37, 38).

CONCLUSIONS

From the results of the present kinetic study performed on the Rh/TiO₂(x% W⁶⁺) catalysts, the following conclusions can be drawn:

1. While the reaction orders with respect to H₂ and CO₂ partial pressures are not significantly altered, CO₂ methanation activity is enhanced by up to 24 times by doping the TiO₂ carrier with less than 1 at.% W⁶⁺.

2. A reduction of apparent activation energy by ca. 25–34 kJ/mol and an improvement of the stability of the catalytic performance are observed upon carrier doping.

3. The rate of gaseous CO formation is found to be affected by carrier doping to a significant extent, via alterations of the CO adsorption capacity and the strength of the Rh–CO bond.

4. The wavenumber of the band due to the linearly adsorbed CO species formed during reaction is found to shift from 2044 to 2058 cm⁻¹ upon carrier doping. Also, the coverage of CO on the supported Rh surface is reduced from ca. 0.30–0.16 upon carrier doping.

5. The induction of the SMSI state results in a significant decrease of the activity of methane formation and a large increase of the activity of CO formation over the Rh/TiO₂(W⁶⁺) catalyst. However, the alteration of the kinetic performance induced by the SMSI phenomenon is reversible during exposure to the reaction mixture.

6. The greatly increased activity caused by doping is found not to be related to the SMSI phenomenon but due to an enhancement of hydrogen adsorption capacity and a weakening of the Rh–CO bond on the catalyst surface.

REFERENCES

1. Schwab, G. M., in "Advances in Catalysis," Vol. 27, p. 1. Academic Press; Orlando, 1978.

2. Solymosi, F., *Catal. Rev.* **1**, 233 (1967).
 3. Baddour, R. F., and Deibert, M. C., *J. Phys. Chem.* **70**, 2173 (1966).
 4. Tauster, S. J., and Fung, S. C., *J. Catal.* **55**, 29 (1978).
 5. Tauster, S. J., Fung, S. C., and Garten, R. L., *J. Am. Chem. Soc.* **100**, 170 (1978).
 6. Kao, C. C., Tsai, S. C., Bahl, M. K., Chung, Y. W., and Lo, W. J., *Surf. Sci.* **95**, 1 (1980).
 7. Burch, R., *J. Catal.* **58**, 220 (1979).
 8. Vannice, M. A., Twu, C. C., and Moon, S. H., *J. Catal.* **79**, 70 (1983).
 9. Akubuiro, E. C., and Verykios, X. E., *J. Catal.* **103**, 320 (1987); **113**, 106 (1988).
 10. Akubuiro, E. C., Ioannides, T., and Verykios, X. E., *J. Catal.* **116**, 590 (1989).
 11. Ioannides, T., and Verykios, X. E., *J. Catal.* **145**, 479 (1994).
 12. Ioannides, T., Verykios, X. E., Tsapatsis, M., and Economou, C., *J. Catal.* **145**, 491 (1994).
 13. Solymosi, F., Tombacz, I., and Koszta, J., *J. Catal.* **95**, 578 (1985).
 14. Ioannides, T., and Verykios, X. E., *J. Catal.* **140**, 353 (1993).
 15. Yang, S. Y., Moon, S. H., and Vannice, M. A., *J. Catal.* **71**, 167 (1981).
 16. Braunschweig, E. J., Logan, A. D., Datye, A. K., and Smith, D. J., *J. Catal.* **118**, 327 (1989).
 17. Solymosi, F., Erdöhelyi, A., and Bansagi, T., *J. Catal.* **68**, 371 (1981).
 18. Araki, M., and Ponec, V., *J. Catal.* **44**, 439 (1976).
 19. Zhang, Z. L., Kladi, A., and Verykios, X. E., *J. Phys. Chem.*, in press.
 20. Akubuiro, E. C., Verykios, X. E., and Ioannides, T., *Appl. Catal.* **46**, 297 (1989).
 21. Prairie, M. R., Renken, A., Highfield, J. G., Thampi, K. R., and Grätzel, M., *J. Catal.* **129**, 130 (1991).
 22. Rethwish, D. G., and Dumesic, J. A., *Langmuir* **2**, 73 (1986).
 23. van't Blik, H. F. J., van Zon, J. B. A. D., Huizinga, T., Vis, J. C., Koningsberger, D. C., and Prins, R., *J. Phys. Chem.* **107**, 3139 (1985).
 24. Solymosi, F., and Pasztor, M., *J. Catal.* **104**, 312 (1987).
 25. Henderson, M. A., and Worley, S. D., *J. Phys. Chem.* **89**, 1417 (1985).
 26. Benites, J. J., Alvero, R., Capitan, M. J., Carrizosa, I., and Odriozola, J. A., *Appl. Catal.* **71**, 219 (1991).
 27. Zhang, Z. L., Kladi, A., and Verykios, X. E., *J. Mol. Catal.*, in press.
 28. Morris, S. R., Moyes, R. B., and Wells, P. B., *Stud. Surf. Sci. Catal.* **11**, 247 (1982).
 29. Bonneviot, L., and Haller, G. L., *J. Catal.* **130**, 359 (1991).
 30. Primet, M., *J. Catal.* **88**, 273 (1984).
 31. Garfunkel, E. L., Farias, M. H., and Somorjai, G. A., *J. Am. Chem. Soc.* **107**, 349 (1985).
 32. Fujita, S., Terunuma, H., Nakamura, M., and Takezawa, N., *Ind. Eng. Chem. Res.* **30**, 1146 (1991).
 33. Peebles, D. E., Goodman, D. W., and White, J. M., *J. Phys. Chem.* **87**, 4378 (1983).
 34. Solymosi, F., Erdöhelyi, A., and Lancz, M., *J. Catal.* **95**, 567 (1985).
 35. Chung, Y. W., Lo, W. J., and Somorjai, G. A., *Surf. Sci.* **64**, 588 (1977).
 36. Weast, R. C., Ed., "Handbook of Chemistry and Physics," 63rd ed. CRS press, Cleveland, 1982–1983.
 37. Trovarelli, A., Mustazza, C., Dolcetti, G., Kaspar, J., and Graziani, M., *Appl. Catal.* **65**, 129 (1990).
 38. Anderson, J. B. F., Burch, R., and Cairns, J. A., *Appl. Catal.* **21**, 179 (1986).